

High Fidelity Simulation of Diesel Engine Spray Atomization Process

Jinghan Zhang

Energy and Power Engineering, North China Electric Power University, Beijing, 102206, China

ABSTRACT. *In this paper, a high-fidelity numerical simulation of the jet crushing and spray formation process of a complex diesel engine injector is performed. For several reasons, the main atomization process of diesel injection has not been fully understood, including the difficulty of entering the optically dense area. Due to the latest advances in numerical methods and computational resources, high-fidelity simulations of real atomized flows are currently feasible, which provides a new mechanism for studying jet rupture processes. In this study, a new fluid volume (VOF) the method is coupled with a random Lagrangian spray (LSP) model to simulate the atomization process. The common rail injector is modeled by the nozzle geometry provided by the engine combustion network (ECN). The operating conditions correspond to a single 90 μ m orifice plate JP-8. The fuel injector operates at 90 bar and 373K, and releases to 100% nitrogen, 29 bar, 300K environment, REL=16,071, Wel=75,334, so that the liquid jet is in an atomized and broken state, use the Army Research Laboratory (ARL). The experimental data set is verified, and the KH-RT breakup model is verified, both of which are related to the spray angle. The droplet distribution of the simulated spray is provided to compare and use the LSP model for future experiments secondary atomization was provided.*

KEYWORDS: *diesel engine, spray atomization, simulation analysis, droplet distribution*

1. Introduction

To date, one of the main bottlenecks in combustion system engineering spray modeling is the accurate description of the main atomization process. Several contemporary numerical solvers use rough approximations in dense areas, based on particles of the size of the injection nozzle, subject to Kelvin-Helmholtz type instability and the influence of Lagrangian particle tracking technology, these methods have achieved great success, but they need to understand the specific spray process to calibrate the model, which makes the theoretical research change impossible [1]. Historically, the development of the main atomization model has been hampered by the well-known difficulties in measuring the optical density spray

area [2]. Although the experimenter has successfully used modern methods such as ballistic imaging and X-ray technology, but it is still not feasible to extract complete four-dimensional information with sufficient spatial and temporal resolution for detailed analysis [3].

The need to accurately model the two-phase atomized flow in high-speed jets is particularly important in diesel injectors, because the mixing quality of fuel and oxidant in diesel injectors is critical for lean combustion [4]. The fuel/air mixture formation is also a very important factor to improve engine efficiency and power density [5]. In order to optimize the design of the combustion chamber, reduce exhaust emissions, and improve combustion performance, the spray and atomization characteristics must be considered. In addition, the geometry of the injector, the injection parameters and the flow mixing in the combustion chamber also affect the diesel spray characteristics [6]. Therefore, the simulation should consider system-level complexity, including real injector characteristics, to accurately predict the true spray dynamics [7].

In the case of a large Weber number, the computational cost of solving all critical length scales is prohibitively high, so the number of detailed numerical simulations conducted under actual diesel engine injector conditions is severely limited [8]. A liquid jet moving at a relative speed of O (100) m/s can produce droplets as small as a few microns in diameter. Therefore, when simulating spray-filled areas, more accurate engineering needs to be established for the primary and secondary crushing modes Broken spray model to reduce the calculation cost.

2. Experimental Method

2.1 Simulation

The simulation in this paper uses the JP-8 fuel property database (373K) to simulate the geometry of the nozzle with an injection pressure of 90 bar, a background pressure of 20 bar, and an outlet speed of 127 m/s. The Reynolds number and Weber number are REL=16,071, respectively. And WEL=75,334. The results show that when the injection pressure is 90 bar, the background pressure is 20 bar, and the outlet speed is 127 m/s, the Reynolds number and Weber number are: Rel=16,071 and Wel=75,334. Determined according to the problem configuration the relative length scale range of the nozzle is from the overall scale of the nozzle orifice ($l_i=d=90\mu\text{m}$) to the viscosity scale ($0.09\mu\text{m}$), and then to the critical radius of Kolmogorov ($0.2\mu\text{m}$). The radius is defined as:

$$l_v = 5.0\text{Re}^{-7/8} \quad \text{and} \quad l_{\text{cr}} = \left(\frac{\sigma^3}{\rho^3 \epsilon^2} \right)^{1/5}$$

In order to deal with the smallest flow structure and improve the calculation efficiency, the dynamic Smagorinsky model of large eddy simulation is used. In the nozzle, the wall analysis method is adopted, and $\Delta x^+, \Delta y^+ \sim 1$ are close to the wall surface (according to LV calculation), $\Delta x^+, \Delta y^+ \sim 50$ are close to the center, and

$\Delta z^+ \sim 70$ (see Figure1). The mesh refinement is essentially Cartesian, forcing $\Delta x = \Delta y = \Delta r$. Use ~ 60 million hexahedrons to control the volume of the discretized area. The dots are concentrated in the jet spray cladding to solve the interface problem, and a thick buffer zone is added in the radial and axial areas to reduce the boundary conditions. Impact (see Figure2). Within the spray envelope, place $\Delta/LCRLSP0.5$ near the undisturbed nominal interface to capture instability, and cover the rest of the spray envelope with $\Delta/LCRLSP40$ to utilize the LSP. The framework achieves savings.

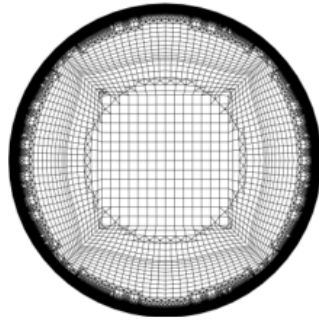


Figure. 1 Grid slice at nozzle outlet

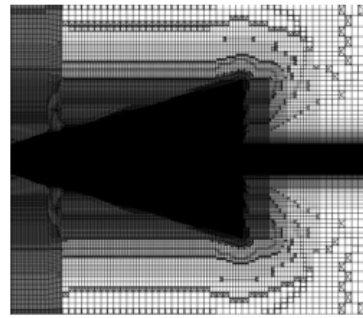


Figure. 2 Grid slice through the centerline of the nozzle

2.2 Experiment

The experiments in this study were conducted in the Army Research Laboratory by injecting a high-speed JP-8 fuel spray into a high-temperature pressure (HTPV) flow chamber. HTPV is designed with a maximum pressure of 150 bar and a maximum temperature of 1000K, using common rail injection the system carries out precise fuel delivery (Kurmann et al. 2014). The vessel is equipped with closed-loop control of pressure and temperature. The flow chamber is kept constant at 58 m³/h. The on-site nitrogen generator produces the nitrogen required for the test. During the period, 99% purity was maintained. To facilitate optical access, the container was equipped with three fused silica windows measuring 147 mm diameter x 85 mm thickness. To protect the 85 mm thick pressure window from fuel contamination, the 85 mm window and a 6 mm thick fused silica window was placed between the spray areas.

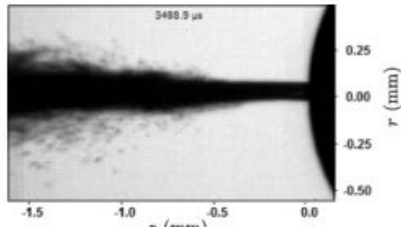


Figure. 3 High-speed near-field imaging under JP-8 spray transition

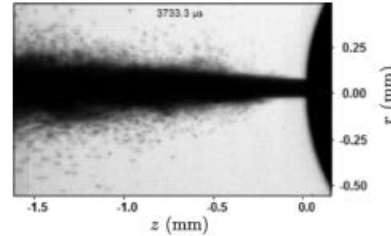


Figure. 4 High-speed near-field image of JP-8 spray in a completely atomized state

A single LED light source and a Photron SA5 camera running at 90,000 fps were used to acquire high-speed near-field spray area images for line-of-sight measurements. For the experiments presented, the image size was set to 320×192 pixels and the corresponding zoom ratio was 5.6μm/Pixel. The sealed chamber conditions are set to 20 bar and 300 K, the specified density ratio is 34. The fuel injection pressure is set to 90 bar, the injection duration is 3 ms, and a total injection mass of 2.2 mg is measured by the IA V injection analyzer. Figures 3 and 4 two examples of spray behavior transition from full fog mode are shown.

2.3 Theoretical Analysis

The Reitz dispersion model was proposed to use aerodynamic parameters to study the spray angle (Reitz & Bracco, 1979). It includes the ratio of the Reynolds number and weber number of the liquid flow in the function $f(\gamma)$ and is written as:

$$\tan(\theta) = \frac{4\pi}{A} \left(\frac{\rho_g}{\rho_l} \right) f(\gamma)$$

Where ρ_g and ρ_l are the liquid and gas density, A is a constant depending on the nozzle design, $A=3.0+0.28l_0/d_0$, d_0 is the nozzle diameter, l_0 is the length of the nozzle of the nozzle diameter. The parameter $f(\gamma)$ is a function of the physical properties of the liquid and the jet velocity.

3. Experimental Results

Nozzle flow turbulence is visualized by sampling the velocity flow field and using the classical Q criterion defined as $Q=1/2(|\Omega_{ij}|-|s_{ij}|)$, and is determined by the velocity component of the flow U Coloring (see Figure 5). The iso-surface of the Q criterion shows the hairpin vortex structure generated by the interaction of the fluid and the wall surface, and the peak velocity of the flow along the center of the pipe flow is larger. Compared with the traditional pipe flow, the vortex's structure is irregular; this difference can be explained by the good pressure gradient of the nozzle and the lack of perfect symmetry in the geometry of the experimental

simulation. However, the newly emerging flow field can be described as turbulent, and the resulting jet rupture. It can be interpreted as being in the area of spray atomization. The combination of turbulent inflow and jet instability leads to chaotic jet behavior, as shown by the flow velocity contour in Figure 6.

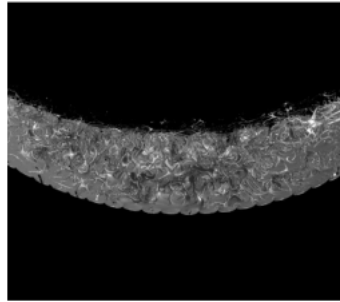


Figure. 5 Seen from the downstream, the q criterion isosurface of the bottom wall of the diesel injector is blocked by the flow velocity

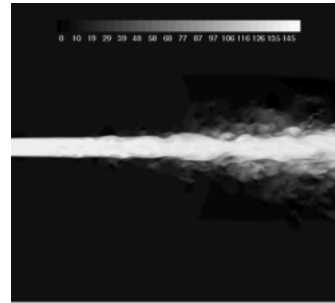


Figure. 6 The contour of the flow velocity (m/s) on the jet center line slice

Figure 7 shows the spray formation process under stable and fully atomized conditions, as shown by the use of $f=0.5$ isosurface and LSP tracking droplets of reference nozzle geometry. Note the increase in hydrodynamic instability and the resulting the generated spray cone. This simulation only models the static fully open valve structure.



Figure. 7 The volume fraction next to the diesel injector is equal to the surface and Lagrangian particles.

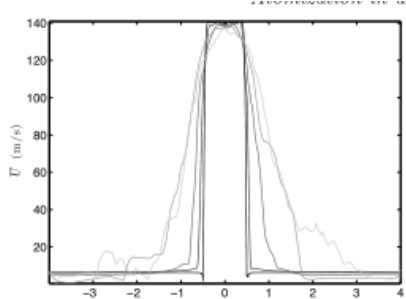


Figure. 8 The function of the average flow velocity and radial distance of the 5 downstream stations: $z/d = \{0,4,8,12,16\}$ (dark to light).

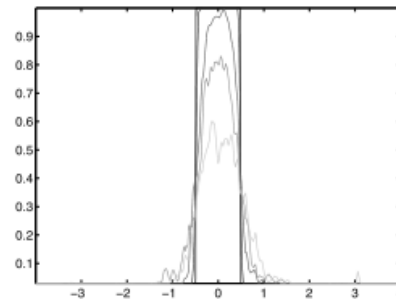


Figure. 9 The average volume fraction of 5 downstream stations (including Lagrangian spray) as a function of radial distance: $z/d = \{0,4,8,12,16\}$ (dark to light).

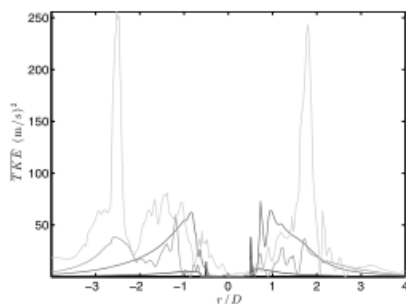


Figure. 10 The function of the average turbulent flow energy of 5 downstream stations and the radial distance: $z/d = \{0,4,8,12,16\}$ (dark to light)

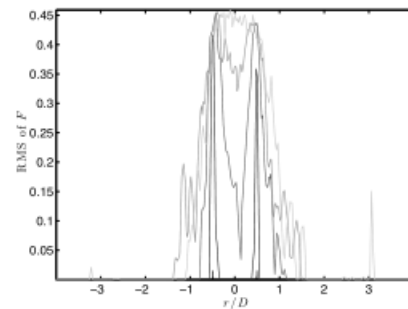


Figure. 11 The function of the root mean square and radial distance of the volume fraction of 5 downstream stations (including Lagrangian spray): $z/d = \{0,4,8,12,16\}$ (dark to light).

Figure 8-11 shows the radial change of the average velocity U and the average volume fraction F with the axial distance. Figure 8 shows the use of a 5% co-current field to stabilize the solution (when $r > D/2$, $U_6 = 0$) and the experimental volume velocity (at $0D$). The U-shaped profile widens downstream, indicating that the number of jets is increasing. Figure 9 shows the F distribution, which includes the equivalent volume fraction of the Lagrange particles. Like U , but to a lesser extent, the F section widens downstream. The F section decreases in height downstream, showing the breakdown and fluctuation of the liquid jet. It is worth noting that the dispersion characteristics between the velocity field and the volume fraction field are very large. The difference shows the entrainment effect of the velocity field and the mass conservation of the volume fraction field. The radial distribution of turbulent flow energy (TKE) is shown in Figure 10. The nozzle tube flow is injected with a sharp TKE peak, which creates a turbulent structure at the fluid interface. It

helps the jet rupture and grow with the shear layer. Figure11 shows the intensity, root mean square (RMS), curve that expands as the shear growth layer grows.

The statistical data does not fully converge, as shown in Figure8, so in order to extract a preliminary estimate of the spray angle θ , we fit a Gaussian curve to each average velocity profile. Figure12 shows a Gaussian fit that is not centered on the origin, it proves that the real geometry lacks axial symmetry (the spray leaves at an angle). Figure13 shows the Gaussian fit to the full width and half height of the average flow direction profile (FWHM); the linear fit to FWHM changes with the axial distance to provide the spray angle θ .

The experimental spray angle is determined by visual observation of 200 spray images (sampling frequency 11.1 μ s), while tracking the interface of the jet core area relative to the jet center line. In the fully atomized spray mode, the total sampling time is equivalent to 2.2ms (Re=16,071, OH=0.017). In order to be consistent with the simulation results, the program does not include the initial transient. The spray angles extracted from Reitz theory, simulation and experiment are:

$$\theta_{\text{Reitz}} = 5.8^\circ, \quad \theta_{\text{sim}} = 5.1^\circ, \quad \text{and} \quad \theta_{\text{exp}} \sim 4^\circ$$

The simulation results are in good agreement with the theoretical dispersion results. However, there is a certain deviation between the experiment with a spray angle of 4° and the experiment with a spray angle of 1°. The difference may be partly due to changes in the nozzle orifice diameter and nozzle shape. These changes are Due to manufacturing eccentricity and cavitation in the nozzle. This difference has been discussed in the previous literature, for ECN type injectors, where geometric inconsistencies are thoroughly reported. The impact of these differences will significantly affect the spray parameter.

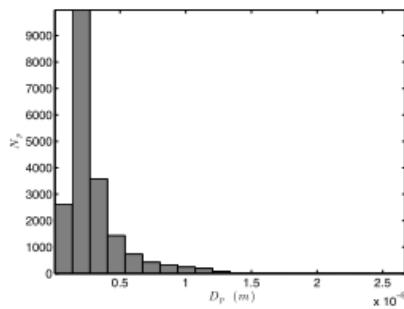


Figure. 12 Number of droplets as a function of diameter

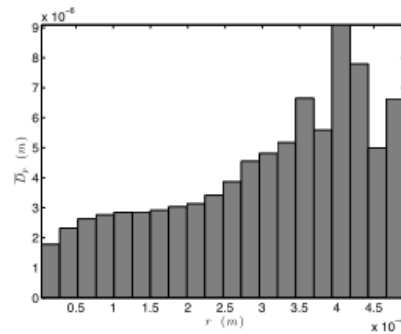


Figure. 13 The average droplet diameter is a function of radial distance

The secondary atomization model requires an initial droplet spray profile, parameterized by the droplet diameter and the distance away from the jet. The droplet size and count are calculated based on the combination of LSP particles and resolved VOF features (for unresolved features, using the same method to transfer

from VOF to LSP, but with a larger number of domain units). Figure12 shows the average number of droplets for a given droplet diameter. The range of droplets is about 1-10 μm , and the average droplet diameter is 3.0 μm , the most likely droplet diameter is 1.5 μm . The droplets <1 μm are spontaneously evaporated and are not tracked. Figure13 shows the average droplet diameter at a given distance from the center of the jet. The average droplet size is far away the area of the nozzle increases, from about 2–7 μm .

4. Conclusion

In this study, the high-fidelity simulation method was used to study the atomization physics of the diesel injector with more detailed internal geometry of the nozzle. The nozzle flow field is described by the Q isosurface that shows the turbulence pattern. Geometry and system dynamics. The complexity of science is characterized by volume fraction isosurfaces and snapshots of Lagrangian droplets. In addition, the average flow velocity and volume fraction statistics also show the structure of high-speed jets. Turbulent flow energy and volume fraction intensity distributions characterize interfacial mixing Process. Comparison with the Reitz spray theory and the measurement results of the flow field near the ARL nozzle shows that the numerical simulation captures the correct dispersion characteristics. The spray size is further characterized by the droplet size and spatial distribution map. At present, further work is in progress, use higher resolution to establish numerical convergence and capture hydrodynamic flow instability for comparison with classical instability models.

Turbulent flow energy and volume fraction intensity distribution characterize the interfacial mixing process. Comparison with the Reitz spray theory and the measurement results of the flow field near the ARL nozzle shows that the numerical simulation captures the correct dispersion characteristics. The spray size and spatial distribution map are used to spray further characterization. Currently, further work is underway to use higher resolution to establish numerical convergence and capture hydrodynamic flow instability for comparison with classical instability models.

References

- [1] Coletti, F., Benson, M. J., Sagues, A. L., Miller, B. H., F ahrig, R. & Eaton, J. K. 2014 Three-dimensional mass fraction distribution of a spray measured by x-ray computed tomography. *J. Eng. Gas Turb. Power* 136, 051508.
- [2] Cummins, S. J., Francois, M. M. & Kothe, D. B. 2005 Estimating curvature from volume fractions. *Computers Structures* 83, 425-434.
- [3] Desjardins, O., Moureau, V. & Pitsch, H. 2008 An accurate conservative level set/ghost fluid method for simulating turbulent atomization. *J. Comput. Phys.* 227, 8395-8416.
- [4] Desjardins, O. & Pitsch, H. 2010 Detailed numerical investigation of turbulent atomization of liquid jets. *Atomization Sprays* 20, 311–336.

- [5] Rong Zhixiang, Xu Huiqiang, Zhou Jianmin. Study on test methods of diesel engine fuel injection atomization and influencing factors of spray performance [J]. *Naval Science and Technology*, 2018, 40 (21): 98-103.
- [6] Hou Yujing. *Effects of High Pressure Injection on Spray, Combustion and Emissions of Light Diesel Engines* [D]. Jilin University, 2016.
- [7] Dong Weitao, Gao Yongqiang, Wang Kewei. Design and application of flash synchronization delay device for diesel engine spray test [J]. *Journal of Wuhan University of Technology (Information and Management Engineering Edition)*, 2016, 38 (01): 640-644.
- [8] Yan Xuesheng. *Study on the Influence of Diesel Engine Nozzle Structure on Spray Characteristics* [D]. Jiangsu University, 2013.